Neuroprotective effect of the alpha 7 nicotinic receptor agonist PHA 543613 in an *in-vivo* excitotoxic adult rat model

Laura Foucault-Fruchard, Aurélie Doméné, Marguerite Windsor, Patrick Emond, Nuno Rodrigues, Frédéric Dollé, Anne Laure Damont, Frédéric Buron, Sylvain Routier, Sylvie Chalon, Daniel Antier.

Published in Neuroscience

doi: 10.1016/j.neuroscience.2017.05.019

Available online 18 May 2017

Neuroprotective effect of the alpha 7 nicotinic receptor agonist PHA 543613 in an *in-vivo* excitotoxic adult rat model

Laura Foucault-Fruchard[1,2,*], Aurélie Doméné[1], Marguerite Windsor[2], Patrick Emond[1], Nuno Rodrigues[3], Frédéric Dollé[4], Anne Laure Damont[4], Frédéric Buron[3], Sylvain Routier[3], Sylvie Chalon[1,§], Daniel Antier[1,2,§].

[§]Contributed equally

[1]UMR INSERM U930, Université François Rabelais, Tours, France

[2]CHRU de Tours, Hôpital Bretonneau, Tours, France

[3]UMR CNRS 7311, Institut de Chimie Organique et Analytique, Université d'Orléans, Orléans, France

[4] CEA, I2BM, Service Hospitalier Frédéric Joliot, Orsay, France

Email addresses:

laura.foucault@univ-tours.fr

aurelie.domene@univ-tours.fr

marguerite.windsor-2@etu.univ-tours.fr

patrick.emond@univ-tours.fr

nuno.rodrigues@univ-orleans.fr

Frederic.DOLLE@cea.fr

annelaure.damont@cea.fr

frederic.buron@univ-orleans.fr

sylvain.routier@univ-orleans.fr

sylvie.chalon@univ-tours.fr

daniel.antier@univ-tours.fr

*Corresponding author: Laura Foucault-Fruchard
UMR INSERM U930
UFR de Médecine,
10 Boulevard Tonnellé,
Tours 37032, France
laura.foucault@univ-tours.fr

Abstract

Background

Neuroinflammation is a key-component of the pathophysiology of neurodegenerative diseases and its regulation, a major therapeutic target to reach since no efficient curative treatment is available. The link between nicotine intake and positive outcome in neurodegenerative diseases has been established suggesting a role played by nicotinic receptors especially the nicotinic acetylcholine receptors α7 (α7nAChRs). The objective of this study was to evaluate *in vivo* the potential dose effects of the PHA 543613, a high affinity agonist of α7nAChRs, on neuron survival and striatal neuroinflammation especially using a radioligand never studied in rat model of brain excitotoxic.

Methods

Twenty-six adult male Wistar rats were lesioned in the right striatum with quinolinic acid (QA) and received either vehicle (Sham group; n=8) or PHA 543613 at a concentration of 6 mg/kg (QA-PHA6; n=8) or 12 mg/kg (QA-PHA12; n=10) intra-peritoneally 1 h before QA lesioning and then twice a day until sacrifice at day-4 post-lesion. The measured kinetic parameters of PHA 543613 in rats were taken into account when the administration schedule was established. A first study compared TSPO quantitative autoradiography in QA-lesioned brains with [^{3}H]DPA-714 and [^{3}H]PK11195 (n=9). The effects of the PHA 543613 on microglia activation and neuronal survival have then been evaluated through [^{3}H]DPA-714 binding and immunofluorescence staining (Ox-42, NeuN) on adjacent brain sections.

Results

We demonstrated that [^{3}H]DPA-714 provide a better signal-to-noise ratio than [^{3}H]PK11195. In addition, we showed that chronic PHA 543613 treatment administered at a dose of 12mg/kg to QA-lesioned rats significantly protected neurons and reduced the intensity of neuroinflammation measured by TSPO and Ox-42 immunostaining.

Conclusions

This study, among the first to evaluate the effects of an α7nAChRs agonist treatment in an excitotoxic model of neuroinflammation with [^{3}H]DPA-714, indicates that PHA 543613 exerts neuroprotective effects on the striatal neurons associated with a reduction in microglial activation. This reinforces the hypothesis that α7nAChRs agonist can provide beneficial effects in the treatment of patients with neurodegenerative diseases through modulation of neuroinflammation.

Keywords

Nicotinic acetylcholine receptors α7 - PHA 543613 - TSPO – Neuroinflammation - DPA-714 - PK-11195 – autoradiography – immunofluorescence – Neurodegeneration

Background

Neuroinflammation is a reaction of the central nervous system in response to infection, injury or trauma. This is a physiological component of innate immunity, which involves a non-specific and early response against a pathogen in order to neutralize and minimize damage at the neuronal level by repairing damaged brain tissue. Microglia-driven neuroinflammation has a beneficial effect on scavenging cell debris, tissue healing and repair. However, during chronic neuroinflammation, activated microglial cells produce pro-inflammatory cytokines, reactive oxygen species and derivatives of nitric oxide (NO) [1]. This activity is responsible for neuronal death by apoptosis which in turn stimulates microglial activation that contributes to the pathophysiology of neurodegenerative diseases [2,3]. Neurons are also able to produce proinflammatory cytokines, complement factors and derivatives of NO. These inflammatory mediators can cause neuronal dysfunction and cell death [4,5].

Neuroinflammation is well known as an important element of brain disorders and in particular neurodegenerative diseases [6].

Regulating neuroinflammation represents therefore a major challenge in the management of patients affected by neurodegenerative diseases such as Alzheimer's, Parkinson's or Huntington's diseases. Nowadays, only symptomatic treatments are available and no curative treatment has a marketing authorization for neurodegenerative diseases. Several lines of research on an anti-inflammatory therapeutic approach have been explored in animal models and in humans, but were all unsuccessful [7–11]. Epidemiological studies have shown that smokers have a lower risk of neurodegenerative diseases than the rest of the population [12–15]. These observations led to an interest in nicotine administration which, by binding to nicotinic acetylcholine receptors, may have beneficial effects on the symptoms of neurodegenerative diseases, particularly Parkinson's disease (PD) [16–20].

Among the different subtypes of nicotinic receptors, the α7 (α7nAChRs) are highly expressed in the mammalian brain particularly by neurons and glial cells [21–23]. They belong to the family of ligand-gated ion channels and have a homopentameric structure of five α7 subunits. α7nAChRs are involved in the control of voluntary movement, memory and attention, sleep

and waking and pain and anxiety. They appear to be involved in a number of brain disorders such as drug addiction, schizophrenia and neurodegenerative diseases like Alzheimer's disease (AD) and PD [21]. It has been shown that α7nAChRs activation improved cognitive functions in several animal models that mimic AD, and the α7nAChRs agonist, EVP-6124, is currently in clinical phase III in mild to moderate AD patients [24]. Additionally, several α7nAChRs agonists are being evaluated for the treatment of PD [25]. First results support the idea that drugs acting at α7nAChRs may be beneficial including one study demonstrating the role of α7nAChRs agonists for the reduction of L-dopa-induced dyskinesias [26-28]. In addition, PNU 282987 and PHA 543613 α7nAChRs agonists have demonstrated neuroprotective and anti-inflammatory effects in different intracerebral haemorrhage models [29,30]. Moreover, these 2 agonists and PNU 120596, an α7nAChRs positive allosteric modulator, have proved the same effect in both *in-vitro* and *in vivo* brain ischemia models [31]. The modulation of the α7nAChRs activation in macrophages influences the synthesis of pro-inflammatory cytokines involved in the regulation of the "cholinergic anti-inflammatory pathway" [32].

PHA 543613 [N- (3R) -1-azabicyclo [2.2.2] - Oct-3- yl- furo [2,3 -c] pyridine -5-carboxamide hydrochloride] is a selective agonist of α7nAChRs, known for its high affinity for α7nAChRs [33,34]. Studies have reported a significant anti-inflammatory effect on primary cultures of neurons and astrocytes (unpublished observations, G. Page). *In vivo*, it improved recognition memory in an AD mouse model [35]. Moreover, promising effects on cognitive function were also observed in a schizophrenia' disease model [33]. Recent study has also demonstrated that PHA 543613 exerts neuroprotective effects on the striatal dopaminergic neurons with a reduction in microglial activation in a PD rat model [28]. Thus, data published in literature relate that therapies targeting glial cells, and more precisely the agonists of α7nAChRs, might provide benefit in neurodegenerative disorders [36]. However, the interactions between the neuroprotective and anti-inflammatory effects are not clearly elucidated. Regarding this question, we used a rat model of acute neuroinflammation obtained by unilateral striatal

injection of quinolinic acid (QA) in which we evaluated the effects of a chronic administration of PHA 543613. QA is a strong agonist of glutamate NMDA (N-methyl-D-aspartate) receptors. Overactivation of NMDA receptors causes a massive intracellular influx of calcium that leads to neuronal death by activation of various enzymes triggering different cell components then leading to neuronal death [37]. Factors released during the death of these neurons rapidly leads to significant microglial activation. This model of Huntington's disease has recently been shown to be useful in studying the overexpression of the translocator protein (TSPO), a marker of neuroinflammation [38-40]. Therefore, the main purpose of the present study was to evaluate *in vivo* the potential dose effects of the selective agonist of α7nAChRs, PHA 543613, on both neuronal survival and microglial activation in a neuroinflammatory excitotoxic rat model using QA intrastriatal injection. We also interested in the effects of repeated administration of PHA 543613 on α7nAChRs density in our rat model of brain excitotoxic. As a secondary goal, the study aimed to carry out autoradiographic quantification of TSPO expression with a radioligand never studied in a rat model of neuroinflammation: the [^{3}H]DPA-714 [41].

Materials and Methods

Animals

All procedures were conducted in accordance with the European Community Council Directive 2010/63/EU for laboratory animal care and the experimental protocol was validated by the Regional Ethical Committee (Authorization N°2015022011523044). Experiments were carried out on 10-week-old normotensive male Wistar rats (CERJ, France) weighing 290–300g at the beginning of experiments. Animals were housed in groups of 2 per cage in a temperature (21 ± 1°C) and humidity (55 ± 5%) controlled environment under a 12-h light/dark cycle, with food and water available *ad libitum*. A total of 39 animals were used for the experiments described below.

Excitotoxic neuroinflammation model

For unilateral striatal QA lesion, rats (n=35) were anaesthetized with isoflurane (Aerrane™, Baxter, France; 4% for induction and 2% for maintenance) and placed in a stereotaxic David Kopf apparatus (tooth bar: -3.3 mm). The animals' body temperature (36.9 ± 0.6°C) was monitored during the surgery by using a thermal probe. The animals were unilaterally injected with 150 nmol of QA (Sigma-Aldrich, Lyon, France), dissolved in 0.1 mol/L phosphate-buffered saline (PBS) pH 7.4, into the right striatum (injection rate: 0.5 µL/min) using a 25 µL microsyringe (Hamilton, Bonaduz, Switzerland) and a micropump (KD Scientific, Holliston, Massachusetts, USA). QA (2 µL) was injected at the following coordinates: AP: + 0.7 mm; ML: - 3 mm; DV: - 5.5 mm from bregma according to Paxinos and Watson [42]. The injection syringe was left in place for an additional 4 min to avoid QA back-flow, and then slowly removed. After surgery, the scalp was sutured and the rats were given buprenorphine (0.05 mg/kg sub-cutaneously) for postoperative pain.

Comparative evaluation of TSPO radioligands [^{3}H]DPA-714 and [^{3}H]PK-11195 by autoradiographic study in QA lesioned rats

We first measured the *in vitro* binding of TSPO by [^{3}H]DPA-714 in comparison to [^{3}H]PK-11195 in adjacent brain sections from 9 QA-lesioned rats. [^{3}H]DPA-714 was prepared according to *Damont and al, 2015* [41] (specific activity 2.1 GBq/µmol) and [^{3}H]PK-11195 was commercially purchased (specific activity 3.06 GBq/µmol; Perkin Elmer, Norwalk, CT, USA). Autoradiographic studies were performed 7 days after QA lesion. After decapitation under isoflurane anesthesia, the brains were carefully removed on ice, then frozen in isopentane cooled at -35°C and stored at -80°C until use. Coronal brain sections 16 µm thick were cut with a cryostat (CM 3050S™, Leica, Germany) at -20°C, collected on gelatinized slides and stored at -80°C for at least 4 days. Brain sections were allowed to equilibrate at room temperature (RT) for 3h, then incubated with 1 nmol/L of labelled ligand ([^{3}H]DPA-714 or [^{3}H]PK-11195) in 50 mmol/L Tris–HCl buffer pH 7.4 at RT for 60 min. Non-specific binding was assessed in the presence of 1 µmol/L stable PK-11195 (Sigma Aldrich, Lyon, France).

Sections were rinsed twice in ice cold buffer (4°C) for 5 min, then briefly in distilled water at 4°C and dried at RT. Dry sections were made conductive by an application of metal electric tape (3M™, Euromedex, Souffelweyersheim, France) on the other side and then placed in the gas chamber of the β-imager™ 2000 (Biospace Lab, Paris, France). Acquisitions were collected over a period of 4 h. Two anatomical regions of interest (ROIs), i.e., the ipsi-lateral (IL) and contra-lateral (CL) striata were selected and identified in Paxinos and Watson atlas [42]. Using the β-vision software (Biospace Lab, Paris, France), the level of bound radioactivity was directly determined by counting the number of β-particles emitted from the delineated area. The radioligand signal in the ROIs was measured for 6 sections per brain and expressed as counts per minute per square millimeter (cpm/mm^2). Specific binding was determined by substracting non-specific binding from total binding. Radioactivity was quantified using an image analyzer (M3-vision™ Biospace Instruments, Paris, France). The percentage increase of TSPO binding in IL *versus* (*vs*) CL hemisphere was calculated as : $\frac{\text{IL-CL}}{\text{CL}} \times 100$

Pharmacokinetics of PHA 543613

Given the lack of data on the pharmacokinetics of PHA 543613, a study to determine the evolution of the concentration *vs* time in plasma and in brain was performed to choose the most suitable dosing regimen and to confirm the PHA 543613 cerebral diffusion. PHA 543613 concentration was measured with ultra liquid chromatography (UHPLC UltiMate® 3000 system, Thermo Scientific Dionex™, Villebon-sur-Yvette, France) coupled with high resolution mass spectrometry (Orbitrap Q exactive™, Thermo Scientific™, Villebon-sur-Yvette, France) in the serum and brain of 4 treated rats after one i.p injection of PHA 543613 at a dose of 6 mg/kg. Blood samples from the jugular vein were collected at 0.5, 1, 3, 6 and 24 h post injection in heparinized tubes. Blood was centrifuged at 2,000 *g*, for 20 min at 4°C, plasma was removed and then kept at -20°C. The rats were killed by decapitation under isoflurane anesthesia. The whole brain was quickly removed and striatum removed and kept

at -80°C. Striatum and plasma were homogeneized respectively in 2 mL and 400 µL of ethyl acetate with internal standard (PHA 568487, Tocris Bioscience, Bristol, UK, 1 µg/mL) and centrifuged at 15,000 *g*, for 5 min at 4°C. Supernatants were removed; ethyl acetate was evaporated. They were filtered and injected into the liquid chromatograph (C18 chromatography). A multistep gradient (followed by a 2 min equilibration time) had a mobile phase A of 0.5% formic acid in water and a mobile phase B of ACN acidified with 0.5% formic acid; the gradient operated at a flow rate of 0.3 mL/min over a run time of 7.5 min. The acquisition and data processing was performed with X-calibur 2.2 (Thermo Scientific™, Villebon-sur-Yvette, France).

Experimental procedure and drug treatment

PHA 543613 hydrochloride (ICOA, Orléans, France) was dissolved in sterile water and intra-peritoneally injected at a concentration of 6 or 12 mg/kg (300 µL/300 g body weight) 1 h before QA lesioning and then twice a day every day until sacrifice at day 4 post-lesion. Twenty six rats were included in this study and separated into 3 groups as follows: 10 lesioned rats received the treatment at 12 mg/kg (QA-PHA12 group), 8 rats received the treatment at 6 mg/kg (QA-PHA6 group) and 8 lesioned rats received intra-peritoneal (i.p) injection of vehicle according to the same administration schedule (Sham group).

Evaluation of PHA 543613 dose-effect on neuroinflammation using TSPO quantification by autoradiography

First we investigated the potential dose-related effect of chronic 4-day treatment with PHA 543613 on striatum expression levels of TSPO. Rodents received either vehicle (n=5) or PHA 543613 at 6 mg/kg (n=8) or 12 mg/kg (n=9) twice a day. In agreement with results previously obtained (see section 3), the density of TSPO binding sites was measured by *in vitro* auroradiographic experiment using [^{3}H]DPA-714 (specific activity 2.1 TBq/mmol ; CEA ; Orsay ; France) as described above. A total of 6 sections per brain were analyzed for each rat. Data from brain sections were collected over 4h with the β-imager™ 2000. Specific

binding (expressed in cpm/mm^2) from 2 ROIs, i.e., IL and CL striatum were determined. Finally, the percentage increase of TSPO binding in IL *vs* CL hemisphere was calculated as :

$$\frac{\text{IL-CL}}{\text{CL}} \times 100$$

Evaluation of PHA 543613 dose-effect on α7nAChRs expression by autoradiography

The density of α7nAChRs binding sites was measured by *in vitro* autoradiography using [^{125}I]α-bungarotoxin (specific activity 81.4 TBq/mmol; Perkin Elmer, Skovlunde, Denmark) on brain sections adjacent to those used in the previous study, in Sham (n=6), QA-PHA6 (n=6) and QA-PHA12 (n=6) rats. Brain sections were allowed to equilibrate at RT for 3h and then were incubated with 0.4 nmol/L of [^{125}I]α-bungarotoxin in 50 mmol/L Tris–HCl buffer pH 7.4 at RT for 60 min. Non-specific binding was assessed in the presence of 1 µmol/L stable α-bungarotoxin (Tocris Bioscience, Bristol, UK). The density of α7nAChRs binding sites was measured as described above (see section 3). A total of 6 sections per brain were analyzed for each rat. Data from brain sections were collected over 4h with the β-imager™ 2000. Specific binding (expressed in cpm/mm^2) from 2 ROIs, i.e., IL and CL striatum was determined.

Evaluation of PHA effects on microglia activation and neuronal survival by immunofluorescence

Immunofluorescence measurements were performed on rats treated by PHA 543613 12 mg/kg (n=6) or vehicle (n=6). Coronal sections (16 µm thick) of striatum adjacent to those used for the autoradiographic study were used for the immunofluorescence staining of neurons (NeuN, MAB377, Millipore, Molsheim, France) and activated microglia (Ox-42, CBL1512, Chemicon International, Temecula, CA, USA). Slices were fixed in 4% paraformaldehyde solution (Sigma, St Quentin Fallavier, France) at RT for 30 min. Tissue sections were washed 3 times in PBS 0.1 mol/L for 5 min at RT and were then incubated for 3 h at RT in a buffer to enhance cell permeability and to block non-specific sites (PBS 0.1

mol/L/0,3%, Triton X-100/5%, normal goat serum). The sections were delineated using the Dako Pen pencil (Z0334 ; Dako, Les Ulis, France) on the glass slide before incubation overnight at 4°C with monoclonal mouse anti-NeuN (1:200) or monoclonal mouse anti-Ox-42 (1:100). Primary antibodies were diluted in PBS 0.1 mol/L/0.3% Triton X-100/1% normal goat serum. After 3 washes with PBS 0.1 mol/L at RT for 5 min, sections were incubated for 1h in a dark box at RT with goat anti-mouse DyLight™ 488 (KPL, Eurobio, Courtaboeuf, France) at 1:500 diluted in PBS/0.3% triton X-100/1% normal goat serum. The slices were washed twice with PBS 0.1 mol/L and twice with distilled water. Then, they were incubated with 4'-6-diamidino-2-phenylindole (DAPI) (0.1 µg/mL) for 15 min. After 3 washings in distilled water, the slices were mounted with fluorescent mounting medium (S3023, DakoCytomation, Trappes, France) and kept at 4°C until observation. Images were acquired with Morpho Strider software (Explora-Nova™, La Rochelle, France) on Leica DM 5500B microscope. Neurons and activated microglia cells were counted with Image J software (Rasband, WS, Image J, US National Institute of Health, Bethesda, Maryland, USA) in 3 areas per striatum for each section and in 2 sections per rat in order to obtain a representative sample of the whole striatum. The number of cells was determined for each rat by calculating the average obtained on the 6 analyzed areas for each hemisphere. Counting was performed by 2 independent operators. The percentage of neuronal loss and of increase of activated microglia in ipsi- *vs* contra-lateral hemisphere were calculated as follows: $\frac{IL-CL}{CL} \times 100$

Statistical Analysis

Results were expressed as mean ± standard error of the mean (SEM). Correlation between the specific binding of TSPO by [^{3}H]PK-11195 and by [^{3}H]DPA-714 was estimated by a two-tailed Spearman test. To compare 2 groups of rats (PHA *vs* Sham), a Mann-Whitney test was used. Comparisons between the binding in the IL and CL sides were performed using the Wilcoxon one-tailed test. The level of significance was $p<0.05$ (GraphPad Prism software version 5, San Diego, CA, USA).

Results

Animals

No physiological issues and no difference in body weight were observed between animals in the Sham, QA-PHA6 and QA-PHA12 groups (on the day of lesion: 300 ± 20 g, 291 ± 4 g and 283 ± 4 g, respectively; at day-4 post-lesion: 278 ± 9 g, 282 ± 2 g and 268 ± 9 g, respectively). Two rats, 1 in the Sham group and 1 in QA-PHA12 group, died on the lesion day.

PHA 543613 quantitative analysis with UHPLC coupled with high resolution mass spectrometry

One hour post-administration of PHA 543613 (6 mg/kg), a peak concentration was observed in serum. Then, the concentration of PHA 543613 rapidly decreased. The rate of PHA 543613 in rat blood decreased by 35 ± 7% and 90 ± 4 % at 2h and 6h post-i.p injection, respectively. At 24h post-administration, PHA 543613 was no longer detectable in serum but was present within striatum. Based on this observation, the rats were treated twice a day at a dose of 6 or 12 mg/kg during the 4 days post-lesion. The first injection was carried out 1h pre-lesion.

Comparative evaluation of TSPO using [^{3}H]DPA-714 and [^{3}H]PK-11195

The comparison of specific binding of TSPO between [^{3}H]PK-11195 and [^{3}H]DPA-714 by autoradiography was performed on brain sections of rats sacrificed 7 days after instrastriatal injection of QA (Fig. 1). Quantification of the autoradiography revealed that the binding of TSPO either by [^{3}H]PK-11195 or [^{3}H]DPA-714 was significantly ($p<0.05$) higher in the IL than in the CL striatum. Non-specific binding in the CL or IL striatum assessed with 1 µmol/L PK11195, was lower with [^{3}H]DPA-714 than with [^{3}H]PK-11195, indicating a better signal-to-noise for [^{3}H]DPA-714 (0.06±0.10 cpm/mm^2 *vs* 0.29±0.02 cpm/mm^2 in CL respectively, $p<0.05$; 0.14 ± 0.02 cpm/mm^2 *vs* 0.37±0.02 cpm/mm^2 in IL respectively; $p<0.05$) (Fig. 1A).

Furthermore, the percentage increase of TSPO specific binding in IL *vs* CL striatum was significantly ($p<0.05$) higher for [^{3}H]DPA-714 than for [^{3}H]PK-11195 (821 ± 70 *vs* 489 ± 42%, respectively) (Fig. 1B). In addition, the percentage increase of TSPO binding in IL *vs* CL striatum was positively correlated using [^{3}H]DPA-714 and [^{3}H]PK-11195 (Fig. 1B, rho= 0.9328, $p<0.05$).

Evaluation of PHA 543613 dose-effect relationship on neuroinflammation using autoradiography

The TSPO density was evaluated on adjacent brain sections using [^{3}H]DPA-714 binding in the IL and CL striatum from each rat in the Sham group and both PHA groups (6 mg/kg and 12 mg/kg) (Fig. 2A). The percentage increase of TSPO binding in IL *vs* CL striatum (Figure 2B) was lower in the QA-PHA6 group than in the Sham group but was not statistically different (764 ± 72%*vs* 967 ± 64%, respectively). However, the percentage increase of TSPO binding in IL *vs* CL striatum was significantly lower in the QA-PHA12 group (731 ± 34% *vs* 967 ± 64%, respectively, $p<0.05$). Finally, the increased rate of TSPO was higher but not statistically different in QA-PHA6 and QA-PHA12 groups.

Evaluation of PHA dose-effect on α7nAChRs expression using autoradiography

The α7nAChRs expression was evaluated on adjacent brain sections by [^{125}I]α-bungarotoxin binding in the IL and CL striatum from each rat in the Sham, QA-PHA6 and QA-PHA12 groups (Fig. 3A). The specific binding of [^{125}I]α- bungarotoxin (Fig. 3B) in the CL side on the one hand and in IL side in the other hand were not significantly different between the Sham, QA-PHA6 and QA-PHA12 groups (1.65 ± 0.42, 1.60 ± 0.26, and 1.83± 0.25 cpm/mm^2 in CL, respectively; 1.36±0.42, 1.11±0.18, and 0.83±0.27 cpm/mm^2 in IL, respectively).

Evaluation of PHA 543613 effect on neuroinflammation by immunofluorescence

The activated microglia were evaluated on adjacent brain sections by Ox-42 marker in the CL and IL striatum in the Sham (n=6) and QA-PHA12 (n=6) groups (Fig. 4A and 4B). In both

groups, Ox-42 staining in IL striatum was significantly ($p<0.05$) increased when compared to CL striatum (Sham: 150 ± 13 cells stained in the IL *vs* 22 ± 2 in the CL side; QA-PHA12: 112 ± 5 cells stained in the IL *vs* 18 ± 1 in the CL side, $p<0.05$) (Fig. 4C). Activated microglia (Ox-42 positive cells) in IL striatum of QA-PHA12 rats were significantly lower (-34%, $p<0.05$) than in Sham. Moreover, activated microglia in IL *vs* CL were lower in the PHA12 group than in Sham (531 ± 107 *vs* 609 ± 77, respectively) (Fig. 4D).

Evaluation of PHA 543613 on neuronal survival by immunofluorescence

Neuron counting was performed on the same rats as above by using NeuN marker (Fig. 5A and 5B). In both groups, NeuN staining was significantly decreased in IL *vs* CL side (QA-PHA12: 114 ± 9 *vs* 206 ± 11 cells in the CL side, $p<0.05$; Sham group: 59 ± 13 *vs* 184 ± 11 cells in the CL side, $p<0.05$) (Fig. 5C). The number of neurons in IL side was 93% higher in the QA-PHA12 group than in the Sham group ($p<0.05$). Moreover, the neuronal loss in IL *vs* CL striatum was significantly lower in the PHA12 than in the Sham group (44.5 ± 4 and 68 ± 7, respectively, $p<0.05$) (Fig. 4D).

Discussion

Neurodegenerative diseases are a major public health problem. Available treatments are only able to improve symptoms, but are unable to slow down or stop the progression of the disease. Many efforts are being deployed for developing such disease-modifying strategies with agents able to have neuroprotective and/or neurorestorative effects. Several studies suggest that neurodegeneration occurs in part because the environment is affected cascade fashion during disease in a cell-autonomous process affecting neurons. This process, called neuroinflammation, is defined by the contributions of glial cells, elements of the blood brain barrier (BBB) or systemic inflammatory processes that can increase the severity of neurodegenerative disease [36]. Thus, these observations indicate that therapies targeting glial cells might provide beneficial effects on neurodegenerative disorders. Downregulation of the activation of microglia can be obtained through the activation of α7nAChRs localized on

392 microglial cells [43]. The agonists of α7nAChRs have been the subjects of several studies on
393 schizophrenia but little data on the treatment of neurodegenerative diseases is published
394 nowadays [44]. Agonists of α7nAChRs appear to be more efficient than acetylcholine at
395 inhibiting the inflammatory signalling and production of pro-inflammatory cytokines from
396 immune cells [45]. However, the effects induced by α7nAChRs stimulation in traumatic brain
397 injury models appear to be either neuroprotective or toxic, highlighting the complexity of the
398 process.
399
400 The present study aimed to improve our knowledge relating to these potential therapeutic
401 targets by evaluating *in vivo* the effects of the selective α7nAChRs agonist PHA 543613, on
402 both neuronal survival and microglial activation in a rodent model of excitotoxic
403 neuroinflammation based on striatal QA injection [39]. PHA 543613 was selected because
404 this compound has already demonstrated neuroprotective and anti-inflammatory effects in
405 different intracerebral haemorrhage models [29,30] and a recent study demonstrated that
406 PHA 543513 exerts neuroprotective effects on the striatal dopaminergic neurons with a
407 reduction in microglial activation in a Parkinson's disease rat model induced by 6-
408 hydroxydopamine (6-OHDA) lesion [28]. A preliminary study allowed us to confirm the ability
409 of this α7nAChRs agonist to pass through the BBB and particularly to evaluate its
410 degradation half-life in order to optimize the drug administration schedule. Therefore, PHA
411 543613 was intra-peritoneally injected 1h before QA lesioning and then twice per day at days
412 1, 2, 3 and 4 post-lesion. The 4-day treatment duration was motivated by recently published
413 data reporting that quick tissue inflammation reached its highest level between day-4 to 7
414 post-QA lesion in this model based on the studied neuroinflammation markers [40,46]. The
415 unilateral intrastriatal injection of QA is admitted as an animal model mimicking the early
416 stages of Huntington's disease. It reproduces some biochemical, behavioural and pathologic
417 features of the disease in rodents and non-human primates [38,47,48]. QA is an endogenous
418 NMDA receptor agonist with excitotoxic properties which is found in normal subjects as a by-
419 product along the kynurenine pathway leading to the synthesis of the essential co-factors

nicotinic acid and nicotinamide adenine dinucleotide [49]. QA spares aspiny striatal interneurons relative to spiny projection neurons [38]. In fact, it acts as a neurotoxin and gliotoxin pro-inflammatory mediator and a pro-oxidant molecule that can alter BBB integrity [50]. Dysfunction of neuronal activity consecutive to the QA injection can induce a pro-inflammatory environment leading to the activation of surrounding microglial cells and in consequence microglial activation. In the chosen excitotoxic model of neuroinflammation, the excessive excitation of NMDA receptors leads to a massive intracellular influx of calcium. This increase is associated with a mitochondrial dysfunction characterized by a decrease of ATP levels that involves the formation and release of reactive oxygen and nitrogen species, thus inducing cell oxidative damage as part of the degenerative process [51]. Moreover, the activation of various enzymes (proteases, lipases and endonucleases) triggering different cell components is also involved in neuronal death [37].

This *in vivo* model of neuroinflammation has been shown to produce large lesions accompanied by an inflammatory response involving increased microglial activation and an axon-sparing neurodegeneration which is directly associated with the degree of brain damage [52,53]. This leads to an increase in the expression of TSPO [39,40,46]. This mitochondrial protein is considered to be a sensitive biomarker of microglial activation [54] and specific imaging tracers are currently used to explore it in preclinical and clinical studies [55-58]. We evaluated this molecular target by quantitative autoradiography. [^{3}H]PK-11195 is a long used tracer in this type of experiment, and the tritiated homolog of the new generation tracer of TSPO, DPA-714, has been recently developed [41]. First, we compared the properties of both of these tracers in our QA rat model and demonstrated that [^{3}H]DPA-714 displayed a lower non specific binding than [^{3}H]PK-11195. This result is in agreement with *in vivo* experiments which observed a higher signal-to-noise ratio using [^{18}F]DPA-714 in comparison to [^{11}C]PK-11195 in different rodent models such as in middle cerebral artery occlusion (MCAO) [59] and herpes encephalitis (HSE) [60]. In addition, higher inter-animal variability in MCAO and HSE models was observed than in our QA model. Thus, we used the

448 tritiated analog of a highly sensitive marker of TSPO that can also be used for *in vivo* human
449 clinical investigations. Then, we examined whether the PHA 543613 effects on TSPO binding
450 with [^{3}H]DPA-714 were dose-related in our model; the compound was administered at the
451 concentrations of 6 mg/kg [28] or 12 mg/kg. The TSPO bindings levels illustrated significant
452 decrease of inflammation in QA-PHA12 *vs* sham animals while the rate of increase of TSPO
453 binding in IL *vs* CL striatum did not decrease significantly between QA-PHA6 and sham
454 group. As a result of this finding and since no difference in body weight or animal
455 comportment were noticed between control, QA-PHA6 and QA-PHA12 animals, we decided
456 to make further experiments with the highest dose of PHA 543613.
457
458 Effects associated to α7nAChRs agonist depend on various parameters like the levels of
459 α7nAChRs expression and function or the neuropathology stage and intrinsic properties of
460 the α7nAChR agonists [61]. α7nAChRs are known to be widely expressed throughout
461 several brain regions in mammals by neurons and glial cells. Among them, the α7nAChRs
462 are probably the most widespread nAChRs subtype expressed in the brain [62]. These
463 receptors can control the release of various types of neurotransmitters, contribute to synaptic
464 plasticity and they have been proved to participate in the regulation of inflammatory reactions
465 [63]. However, the rapid desensitization of α7nAChRs is considered an important factor
466 limiting its potential therapeutic use. Therefore, to approach the mechanism that could
467 explain the beneficial effect of PHA 543613 on neuroinflammation, we quantified α7nAChRs
468 expression in both IL and CL striata of Sham, PHA 6mg/kg and PHA 12mg/kg QA-lesioned
469 animals. Autoradiography binding with alpha-bungarotoxin was performed at 4-days post-
470 lesion and confirmed the expression of α7nAChRs in the striatum of all groups of rats. In
471 addition, we observed a decreasing of binding in IL *vs* CL striatum in Sham, PHA6 and
472 PHA12 rats, hypothetically reflecting the tissue destruction and thus neuron and glial cell loss
473 induced in all animals by local QA injection. This result could also be consistent with a recent
474 publication reporting that neuroinflammation induced by regular bacterial lipopolysaccharide
475 injections resulted in the decrease of α7nAChRs density in the brain of mice [64]. Indeed,

after activation, the α7nAChRs undergo rapid desensitivation in order to limit the influx of calcium (Ca^{2+}) into the cell which could lead to a phenomenon of excitotoxicity [65]. However, 4-day chronic treatment with PHA 543613 did not lead to a significant modification of α7nAChRs expression *vs* control which reveals no significant receptor desensitivation. This observation probably does not apply to our short-term PHA exposure suggesting no induced receptor desensitivation. Lastly, it is then noteworthy that in spite of the diminution of α7nAChRs expression in lesioned striatum of PHA12-treated animals, neuroprotective and anti-inflammatory effects of the drug were observed.

The effects of the PHA 543613 treatment on microglial activation in striatum were also assessed by immunohistochemistry using Ox-42 - an antibody specific to CD11b mostly expressed in activated microglia. Measurements showed in both QA-PHA12 and Sham groups a significant massive increase of Cd11b expression in the striatum from the IL hemisphere *vs* CL hemisphere, confirming the inflammatory impact of QA injection on microglial cell activity. Interestingly, the number of cells expressing the CD11b was significantly (-25.5%) lower in IL striatum of QA-PHA12 rats than in IL striatum of Sham rats. To evaluate the potential effect of PHA543613 treatment on neuron survival in striatum, we used Neun marker located in the nucleus and the perinuclear cytoplasm of postmitotic neurons in mammals. We logically observed significant reduction in neuron population in IL striatum *vs* CL of both QA-PHA12 and Sham groups, illustrating once again the deleterious effect of QA injected locally. However, considering IL striatum counting of both QA-PHA12 and Sham rats, it is noteworthy that the number of preserved neurons was approximately twice as high in the QA-PHA12 than in the Sham group, illustrating the protective effect mediated by PHA treatment in IL striatum of treated animals. Those results indicate that the neuroprotective effects on the striatal neurons are associated with a reduction in microglial activation. Although QA exerts the greatest damage to neurons where NMDA receptors are present, cholinergic and GABAergic neuronal cell types seem to be more sensitive than others especially in the striatum [49,66]. Thus, these two types of neurons do not seem to be

involved in the beneficial effects observed following administration of PHA 543613 in our study.

We report here through the first evaluation of the α7nAChRs agonist PHA 543613 in an *in vivo* excitotoxic model of neuroinflammation, the strong relationship that exists between the effects of PHA 543613 on neuroinflammation and neuron integrity. We confirm that PHA 543613 can reduce both neuronal loss and microglial activation in the same animals, as already observed in a rat model of Parkinson's disease [28]. The α7nAChRs are able to mediate the anti-inflammatory effect of acetylcholine by attenuating the pro-inflammatory cytokine release involved in the regulation of the cholinergic anti-inflammatory pathway in brain astrocytes or microglia [67]. However, α7nAChRs chronic stimulation has been associated with massive and persistent calcium increase inside brain cells well known to be toxic to cells expressing this receptor [68]. This statement supports the necessity to pay attention to the duration of α7nAChRs agonist regimen when used for a therapeutic purpose. Indeed, we have demonstrated the capability of a α7nAChRs-activating agent to induce fast neuroprotection facing an acute brain traumatic injury; these findings support the short-term use of α7nAChRs-activating agents as a strategy to reduce traumatic brain injury triggered BBB permeability [69]. Considering that PHA 543613 can target both of the processes involved in most neurodegenerative diseases, α7nAChRs agonists could represent a major therapeutic challenge in neurology.

List of abbreviations

AD: Alzheimer disease

BBB: blood brain barrier

CL: contra lateral

cpm: counts per min

HSE: herpes encephalitis

IL: ipsi lateral

i.p: intraperitoneal

α7nAChRs: nicotinic acetylcholine receptor α7

MCAO: middle cerebral artery occlusion

NeuN: neuronal nuclei

NMDA: N-methyl-D-aspartate

NO: nitric oxyde

PD: Parkinson disease

QA: quinolinic acid

ROIs: regions of interest

RT: room temperature

SEM: standard error of the mean

TSPO: 18kDa translocator protein

Vs: versus

Ethics approval

All procedures were conducted in accordance with the European Community Council Directive 2010/63/EU for laboratory animal care and the experimental protocol was validated by the Regional Ethical Committee (Authorization N°2015022011523044).

Competing interest

The authors declare that they have no competing interests.

Authors' contributions

SC and DA contributed equally to this work.

Availability of data and materials

The datasets during and/or analysed during the current study available from the corresponding author on reasonable request.

Aknowledgements

This work was supported by the Région Centre-Val de Loire (2014 00094049 - AP 2014-850) and the European Union's Seventh Framework Programme (FP7/2007-2013) under grant agreement n°278850 (INMiND). Authors thank Sylvie Bodard and Zuhal Gulhan for technical assistance.

Consent for publication

Not applicable

Funding

Not applicable

588 **References**

589 1. Takahashi K, Funata N, Ikuta F, Sato S. Neuronal apoptosis and inflammatory
590 responses in the central nervous system of a rabbit treated with Shiga toxin-2. J
591 Neuroinflammation. 2008;5:11.

592 2. Block ML, Hong J-S. Microglia and inflammation-mediated neurodegeneration: multiple
593 triggers with a common mechanism. Prog Neurobiol. 2005 Jun;76(2):77–98.

594 3. Smith JA, Das A, Ray SK, Banik NL. Role of pro-inflammatory cytokines released from
595 microglia in neurodegenerative diseases. Brain Res Bull. 2012 Jan 4;87(1):10–20.

596 4. Haynes SE, Hollopeter G, Yang G, Kurpius D, Dailey ME, Gan W-B, et al. The P2Y12
597 receptor regulates microglial activation by extracellular nucleotides. Nat Neurosci. 2006
598 Dec;9(12):1512–9.

599 5. Hoozemans JJM, Veerhuis R, Rozemuller AJM, Arendt T, Eikelenboom P. Neuronal
600 COX-2 expression and phosphorylation of pRb precede p38 MAPK activation and
601 neurofibrillary changes in AD temporal cortex. Neurobiol Dis. 2004 Apr;15(3):492–9.

602 6. Glass CK, Saijo K, Winner B, Marchetto MC, Gage FH. Mechanisms Underlying
603 Inflammation in Neurodegeneration. Cell. 2010 Mar 19;140(6):918–34.

604 7. Bartels AL, Willemsen ATM, Doorduin J, de Vries EFJ, Dierckx RA, Leenders KL. [11C]-
605 PK11195 PET: quantification of neuroinflammation and a monitor of anti-inflammatory
606 treatment in Parkinson's disease? Parkinsonism Relat Disord. 2010 Jan;16(1):57–9.

607 8. Gordon PH, Moore DH, Miller RG, Florence JM, Verheijde JL, Doorish C, et al. Efficacy
608 of minocycline in patients with amyotrophic lateral sclerosis: a phase III randomised
609 trial. Lancet Neurol. 2007 Dec;6(12):1045–53.

610 9. Huntington Study Group DOMINO Investigators. A futility study of minocycline in
611 Huntington's disease. Mov Disord Off J Mov Disord Soc. 2010 Oct 15;25(13):2219–24.

612 10. Relkin N. Clinical trials of intravenous immunoglobulin for Alzheimer's disease. J Clin
613 Immunol. 2014 Jul;34 Suppl 1:S74-79.

614 11. Zhang Y, Metz LM, Yong VW, Bell RB, Yeung M, Patry DG, et al. Pilot study of
615 minocycline in relapsing-remitting multiple sclerosis. Can J Neurol Sci J Can Sci Neurol.
616 2008 May;35(2):185–91.

617 12. Gotti C, Clementi F. Neuronal nicotinic receptors: from structure to pathology. Prog
618 Neurobiol. 2004 Dec;74(6):363–96.

619 13. O'Reilly EJ, McCullough ML, Chao A, Jane Henley S, Calle EE, Thun MJ, et al.
620 Smokeless tobacco use and the risk of Parkinson's disease mortality. Mov Disord. 2005
621 Oct 1;20(10):1383–4.

622 14. Searles Nielsen S, Gallagher LG, Lundin JI, Longstreth W t., Smith-Weller T, Franklin
623 GM, et al. Environmental tobacco smoke and Parkinson's disease. Mov Disord. 2012
624 Feb 1;27(2):293–7.

625 15. Thacker EL, O'Reilly EJ, Weisskopf MG, Chen H, Schwarzschild MA, McCullough ML,
626 et al. Temporal relationship between cigarette smoking and risk of Parkinson disease.
627 Neurology. 2007 Jun 3;68(10):764–8.

628 16. Newhouse P, Kellar K, Aisen P, White H, Wesnes K, Coderre E, et al. Nicotine
629 treatment of mild cognitive impairment: a 6-month double-blind pilot clinical trial.
630 Neurology. 2012 Jan 10;78(2):91–101.

631 17. Villafane G, Cesaro P, Rialland A, Baloul S, Azimi S, Bourdet C, et al. Chronic high
632 dose transdermal nicotine in Parkinson's disease: an open trial. Eur J Neurol. 2007 Dec
633 1;14(12):1313–6.

18. Itti E, Villafane G, Malek Z, Brugières P, Capacchione D, Itti L, et al. Dopamine transporter imaging under high-dose transdermal nicotine therapy in Parkinson's disease: an observational study. Nucl Med Commun. 2009 Jul;30(7):513–8.

19. Holmes AD, Copland DA, Silburn PA, Chenery HJ. Acute nicotine enhances strategy-based semantic processing in Parkinson's disease. Int J Neuropsychopharmacol Off Sci J Coll Int Neuropsychopharmacol CINP. 2011 Aug;14(7):877–85.

20. Vieregge A, Sieberer M, Jacobs H, Hagenah JM, Vieregge P. Transdermal nicotine in PD A randomized, double-blind, placebo-controlled study. Neurology. 2001 Sep 25;57(6):1032–5.

21. Dineley KT, Pandya AA, Yakel JL. Nicotinic ACh receptors as therapeutic targets in CNS disorders. Trends Pharmacol Sci. 2015 Feb;36(2):96–108.

22. Gahring LC, Persiyanov K, Dunn D, Weiss R, Meyer EL, Rogers SW. Mouse strain-specific nicotinic acetylcholine receptor expression by inhibitory interneurons and astrocytes in the dorsal hippocampus. J Comp Neurol. 2004 Jan 12;468(3):334–46.

23. Jensen AA, Frølund B, Liljefors T, Krogsgaard-Larsen P. Neuronal nicotinic acetylcholine receptors: structural revelations, target identifications, and therapeutic inspirations. J Med Chem. 2005 Jul 28;48(15):4705–45.

24. Prickaerts J, van Goethem NP, Chesworth R, Shapiro G, Boess FG, Methfessel C, et al. EVP-6124, a novel and selective α7 nicotinic acetylcholine receptor partial agonist, improves memory performance by potentiating the acetylcholine response of α7 nicotinic acetylcholine receptors. Neuropharmacology. 2012 Feb;62(2):1099–110.

25. Quik M, Zhang D, McGregor M, Bordia T. Alpha7 nicotinic receptors as therapeutic targets for Parkinson's disease. Biochem Pharmacol. 2015 Oct 15;97(4):399–407.

657 26. Bordia T, McGregor M, Papke RL, Decker MW, Michael McIntosh J, Quik M. The α7
658 nicotinic receptor agonist ABT-107 protects against nigrostriatal damage in rats with
659 unilateral 6-hydroxydopamine lesions. Exp Neurol. 2015 Jan;263:277–84.

660 27. Di Paolo T, Grégoire L, Feuerbach D, Elbast W, Weiss M, Gomez-Mancilla B. AQW051,
661 a novel and selective nicotinic acetylcholine receptor α7 partial agonist, reduces l-Dopa-
662 induced dyskinesias and extends the duration of l-Dopa effects in parkinsonian
663 monkeys. Parkinsonism Relat Disord. 2014 Nov;20(11):1119–23.

664 28. Sérrière S, Doméné A, Vercouillie J, Mothes C, Bodard S, Rodrigues N, et al.
665 Assessment of the Protection of Dopaminergic Neurons by an α7 Nicotinic Receptor
666 Agonist, PHA 543613 Using [(18)F]LBT-999 in a Parkinson's Disease Rat Model. Front
667 Med. 2015;2:61.

668 29. Krafft PR, Altay O, Rolland WB, Duris K, Lekic T, Tang J, et al. α7 Nicotinic
669 Acetylcholine Receptor Agonism Confers Neuroprotection Through GSK-3β Inhibition in
670 a Mouse Model of Intracerebral Hemorrhage. Stroke. 2012 Jan 3;43(3):844–50.

671 30. Krafft PR, Caner B, Klebe D, Rolland WB, Tang J, Zhang JH. PHA-543613 preserves
672 blood-brain barrier integrity after intracerebral hemorrhage in mice. Stroke J Cereb Circ.
673 2013 Jun;44(6):1743–7.

674 31. Barrio L del, Martín-de-Saavedra MD, Romero A, Parada E, Egea J, Avila J, et al.
675 Neurotoxicity Induced by Okadaic Acid in the Human Neuroblastoma SH-SY5Y Line
676 Can Be Differentially Prevented by α7 and β2* Nicotinic Stimulation. Toxicol Sci. 2011
677 Jan 9;123(1):193–205.

678 32. Rosas-Ballina M, Ochani M, Parrish WR, Ochani K, Harris YT, Huston JM, et al. Splenic
679 nerve is required for cholinergic antiinflammatory pathway control of TNF in
680 endotoxemia. Proc Natl Acad Sci U S A. 2008 Aug 5;105(31):11008–13.

681 33. Wishka DG, Walker DP, Yates KM, Reitz SC, Jia S, Myers JK, et al. Discovery of N-
682 [(3R)-1-azabicyclo[2.2.2]oct-3-yl]furo[2,3-c]pyridine-5-carboxamide, an agonist of the
683 alpha7 nicotinic acetylcholine receptor, for the potential treatment of cognitive deficits in
684 schizophrenia: synthesis and structure--activity relationship. J Med Chem. 2006 Jul
685 13;49(14):4425–36.

686 34. Acker BA, Jacobsen EJ, Rogers BN, Wishka DG, Reitz SC, Piotrowski DW, et al.
687 Discovery of N-[(3R,5R)-1-azabicyclo[3.2.1]oct-3-yl]furo[2,3-c]pyridine-5-carboxamide
688 as an agonist of the alpha7 nicotinic acetylcholine receptor: in vitro and in vivo activity.
689 Bioorg Med Chem Lett. 2008 Jun 15;18(12):3611–5.

690 35. Sadigh-Eteghad S, Mahmoudi J, Babri S, Talebi M, Sadigh-Eteghad S, Mahmoudi J, et
691 al. Effect of alpha-7 nicotinic acetylcholine receptor activation on beta-amyloid induced
692 recognition memory impairment. Possible role of neurovascular function. Acta Cir Bras.
693 2015 Nov;30(11):736–42.

694 36. Ransohoff RM. How neuroinflammation contributes to neurodegeneration. Science.
695 2016 Aug 19;353(6301):777–83.

696 37. Estrada Sánchez AM, Mejía-Toiber J, Massieu L. Excitotoxic neuronal death and the
697 pathogenesis of Huntington's disease. Arch Med Res. 2008 Apr;39(3):265–76.

698 38. Schwarcz R, Köhler C. Differential vulnerability of central neurons of the rat to quinolinic
699 acid. Neurosci Lett. 1983 Jul 15;38(1):85–90.

700 39. Arlicot N, Katsifis A, Garreau L, Mattner F, Vergote J, Duval S, et al. Evaluation of
701 CLINDE as potent translocator protein (18 kDa) SPECT radiotracer reflecting the
702 degree of neuroinflammation in a rat model of microglial activation. Eur J Nucl Med Mol
703 Imaging. 2008 Dec;35(12):2203–11.

40. Arlicot N, Tronel C, Bodard S, Garreau L, de la Crompe B, Vandevelde I, et al. Translocator protein (18 kDa) mapping with [125I]-CLINDE in the quinolinic acid rat model of excitotoxicity: a longitudinal comparison with microglial activation, astrogliosis, and neuronal death. Mol Imaging. 2014;13:4–11.

41. Damont A, Garcia-Argote S, Buisson D-A, Rousseau B, Dollé F. Efficient tritiation of the translocator protein (18 kDa) selective ligand DPA-714. J Label Compd Radiopharm. 2015 Jan;58(1):1–6.

42. Dr GP, Watson C. The Rat Brain in Stereotaxic Coordinates: Compact. 6th ed. Academic Press; 2008.

43. Shytle RD, Mori T, Townsend K, Vendrame M, Sun N, Zeng J, et al. Cholinergic modulation of microglial activation by alpha 7 nicotinic receptors. J Neurochem. 2004 Apr;89(2):337–43.

44. Kalkman HO, Feuerbach D. Modulatory effects of α7 nAChRs on the immune system and its relevance for CNS disorders. Cell Mol Life Sci CMLS. 2016 Jul;73(13):2511–30.

45. de Jonge WJ, Ulloa L. The alpha7 nicotinic acetylcholine receptor as a pharmacological target for inflammation. Br J Pharmacol. 2007 Aug;151(7):915–29.

46. Moresco RM, Lavazza T, Belloli S, Lecchi M, Pezzola A, Todde S, et al. Quinolinic acid induced neurodegeneration in the striatum: a combined in vivo and in vitro analysis of receptor changes and microglia activation. Eur J Nucl Med Mol Imaging. 2008 Apr;35(4):704–15.

47. Alexi T, Borlongan CV, Faull RL, Williams CE, Clark RG, Gluckman PD, et al. Neuroprotective strategies for basal ganglia degeneration: Parkinson's and Huntington's diseases. Prog Neurobiol. 2000 Apr;60(5):409–70.

48. Beal MF, Kowall NW, Ellison DW, Mazurek MF, Swartz KJ, Martin JB. Replication of the neurochemical characteristics of Huntington's disease by quinolinic acid. Nature. 1986 May 8;321(6066):168–71.

49. Pérez-De La Cruz V, Königsberg M, Santamaría A. Kynurenine pathway and disease: an overview. CNS Neurol Disord Drug Targets. 2007 Dec;6(6):398–410.

50. Guillemin GJ. Quinolinic acid, the inescapable neurotoxin. FEBS J. 2012 Apr;279(8):1356–65.

51. Nicholls DG. Mitochondrial dysfunction and glutamate excitotoxicity studied in primary neuronal cultures. Curr Mol Med. 2004 Mar;4(2):149–77.

52. Kreutzberg GW. Microglia: a sensor for pathological events in the CNS. Trends Neurosci. 1996 Aug;19(8):312–8.

53. Heneka MT, Rodríguez JJ, Verkhratsky A. Neuroglia in neurodegeneration. Brain Res Rev. 2010 May;63(1–2):189–211.

54. Chen M-K, Guilarte TR. Translocator protein 18 kDa (TSPO): molecular sensor of brain injury and repair. Pharmacol Ther. 2008 Apr;118(1):1–17.

55. Venneti S, Lopresti BJ, Wiley CA. The peripheral benzodiazepine receptor (Translocator protein 18kDa) in microglia: from pathology to imaging. Prog Neurobiol. 2006 Dec;80(6):308–22.

56. Chauveau F, Van Camp N, Dollé F, Kuhnast B, Hinnen F, Damont A, et al. Comparative evaluation of the translocator protein radioligands 11C-DPA-713, 18F-DPA-714, and 11C-PK11195 in a rat model of acute neuroinflammation. J Nucl Med Off Publ Soc Nucl Med. 2009 Mar;50(3):468–76.

749 57. Corcia P, Tauber C, Vercoullie J, Arlicot N, Prunier C, Praline J, et al. Molecular
750 imaging of microglial activation in amyotrophic lateral sclerosis. PloS One.
751 2012;7(12):e52941.

752 58. Hamelin L, Lagarde J, Dorothée G, Leroy C, Labit M, Comley RA, et al. Early and
753 protective microglial activation in Alzheimer's disease: a prospective study using 18F-
754 DPA-714 PET imaging. Brain J Neurol. 2016 Apr;139(Pt 4):1252–64.

755 59. Boutin H, Prenant C, Maroy R, Galea J, Greenhalgh AD, Smigova A, et al. [18F]DPA-
756 714: direct comparison with [11C]PK11195 in a model of cerebral ischemia in rats. PloS
757 One. 2013;8(2):e56441.

758 60. Doorduin J, Klein HC, Dierckx RA, James M, Kassiou M, de Vries EFJ. [11C]-DPA-713
759 and [18F]-DPA-714 as new PET tracers for TSPO: a comparison with [11C]-(R)-
760 PK11195 in a rat model of herpes encephalitis. Mol Imaging Biol MIB Off Publ Acad Mol
761 Imaging. 2009 Dec;11(6):386–98.

762 61. Shen J, Wu J. Nicotinic Cholinergic Mechanisms in Alzheimer's Disease. Int Rev
763 Neurobiol. 2015;124:275–92.

764 62. Zoli M, Pistillo F, Gotti C. Diversity of native nicotinic receptor subtypes in mammalian
765 brain. Neuropharmacology. 2015 Sep;96(Pt B):302–11.

766 63. Soria-Fregozo C, Flores-Soto ME, Pérez-Vega MI, Feria-Velasco A. 5-HT denervation
767 of the adult rat prefrontal cortex induces changes in the expression of α4 and α7
768 nicotinic acetylcholine receptor subtypes. Neurol Barc Spain. 2013 May;28(4):212–8.

769 64. Lykhmus O, Gergalova G, Zouridakis M, Tzartos S, Komisarenko S, Skok M.
770 Inflammation decreases the level of alpha7 nicotinic acetylcholine receptors in the brain
771 mitochondria and makes them more susceptible to apoptosis induction. Int
772 Immunopharmacol. 2015 Nov;29(1):148–51.

65. Zhang Z, Vijayaraghavan S, Berg DK. Neuronal acetylcholine receptors that bind α-bungarotoxin with high affinity function as ligand-gated ion channels. Neuron. 1994 Jan 1;12(1):167–77.

66. Lugo-Huitrón R, Ugalde Muñiz P, Pineda B, Pedraza-Chaverrí J, Ríos C, Pérez-de la Cruz V. Quinolinic acid: an endogenous neurotoxin with multiple targets. Oxid Med Cell Longev. 2013;2013:104024.

67. Stuckenholz V, Bacher M, Balzer-Geldsetzer M, Alvarez-Fischer D, Oertel WH, Dodel RC, et al. The α7 nAChR agonist PNU-282987 reduces inflammation and MPTP-induced nigral dopaminergic cell loss in mice. J Park Dis. 2013;3(2):161–72.

68. Williams DK, Peng C, Kimbrell MR, Papke RL. Intrinsically low open probability of α7 nicotinic acetylcholine receptors can be overcome by positive allosteric modulation and serum factors leading to the generation of excitotoxic currents at physiological temperatures. Mol Pharmacol. 2012 Oct;82(4):746–59.

69. Dash PK, Zhao J, Kobori N, Redell JB, Hylin MJ, Hood KN, et al. Activation of Alpha 7 Cholinergic Nicotinic Receptors Reduce Blood-Brain Barrier Permeability following Experimental Traumatic Brain Injury. J Neurosci Off J Soc Neurosci. 2016 Mar 2;36(9):2809–18.

Figure legends

Figure 1: Comparative evaluation of TSPO radioligands [^{3}H]DPA-714 and [^{3}H]PK-11195 by autoradiographic study. (**A**) Representative autoradiographic images obtained on 16 µm-thick coronal brain sections with [^{3}H]PK-11195 (1 nmol/L, left panel) and [^{3}H]DPA-714 (1 nmol/L, right panel) alone or in presence of stable PK11195 (1 µmol/L, in the right of each panel) of the same animal.(**B**) Percentage of TSPO specific binding in IL *vs* CL striatum (mean % ± SEM) from QA lesioned rats (n= 9) with [^{3}H]PK-11195 or [^{3}H]DPA-714. (**C**) Correlation between [^{3}H]PK-11195 and [^{3}H]DPA-714 autoradiography study. The correlation is reported for the percentage of TSPO binding in IL *vs* CL striatum with each tracer. #p<0.05 (Mann Whitney test). *p<0.05 (two-tailed Spearman test). Abbreviations: CL: contralateral; IL: ipsilateral: SEM: standard error of the mean.

Figure 2: Autoradiographic analysis of TSPO density with [^{3}H]DPA-714 in the striatum. (**A**) Representative total (left side) and non-specific (right side) binding of [^{3}H]DPA-714 obtained on 16 µm-thick coronal brain section in Sham rats (upper panel), QA-PHA 6 and QA-PHA12 rats (lower panel). (**B**) Percentage increase of TSPO binding in IL *vs* CL striatum (mean % ± SEM) from Sham (n= 5), QA-PHA6 (n= 8) and QA-PHA12 (n= 9) rats. Abbreviations: CL: contralateral; IL: ipsilateral: SEM: standard error of the mean.

Figure 3: Autoradiographic analysis of α7nAChRs density with [^{125}I]α-bungarotoxin in the striatum. (**A**) Representative total (left side) and non-specific (right side) binding of [^{125}I]α-bungarotoxin obtained on 16 µm-thick coronal brain section in Sham rats (upper panel), QA-PHA 6 and QA-PHA12 rats (lower panel). (**B**) α7nAChRs expression in IL and CL striatum from Sham (n=6), QA-PHA6 (n=6) and QA-PHA12 (n=6) rats. Data are expressed as cpm/mm^2. Abbreviations : CL: contralateral; IL: ipsilateral; cpm/mm^2: counts per min per mm^2.

Figure 4: Immunofluorescence in rat striatum of Ox-42 in Sham group and QA-PHA12 group. (**A**) Coronal rat brain representation. The full line and areas marked in red symbolize, respectively, the site of injury and areas where Ox-42 immunofluorescence was performed. (**B**) Representative immunofluorescence images of activated microglia by Ox-42 staining (green channel) and DAPI (blue channel) in the CL (left) and IL (right) striatum of Sham (upper) (n=6) and QA-PHA12 (lower) (n=6) rats. Magnification was x 20. Scale bar, 50 µm. (**C**) Ox-42 expression in IL and CL striatum for each group. Data are expressed as number of cells expressing Ox-42 marker. (D) Data are expressed as relative activated microglia in IL *vs* CL striatum for each group. # $p<0.05$ (Mann Whitney test). ∗ $p<0.05$ (Wilcoxon test). Abbreviations: CL: contralateral; IL: ipsilateral.

Figure 5: Immunofluorescence in rat striatum of neurons (NeuN) in Sham group and QA-PHA12 group. (A) Coronal rat brain representation. The full line and areas marked in red symbolize, respectively, the site of injury and areas where NeuN immunofluorescence was performed. (B) Representative immunofluorescence images of neurons by NeuN staining (green channel) and DAPI (blue channel) in the CL (left) and IL (right) striatum of Sham (upper) (n=6) and QA-PHA12 (lower) (n=6) rats. (C) Neuronal expression in CL and IL striatum for each group. Data are expressed as number of cells expressing NeuN marker. (D) Data are expressed as relative neuronal loss in IL *vs* CL striatum for each group # $p<0.05$ (Mann Whitney test). ∗ $p<0.05$ (Wilcoxon test). Abbreviations: CL: contralateral; IL: ipsilateral.

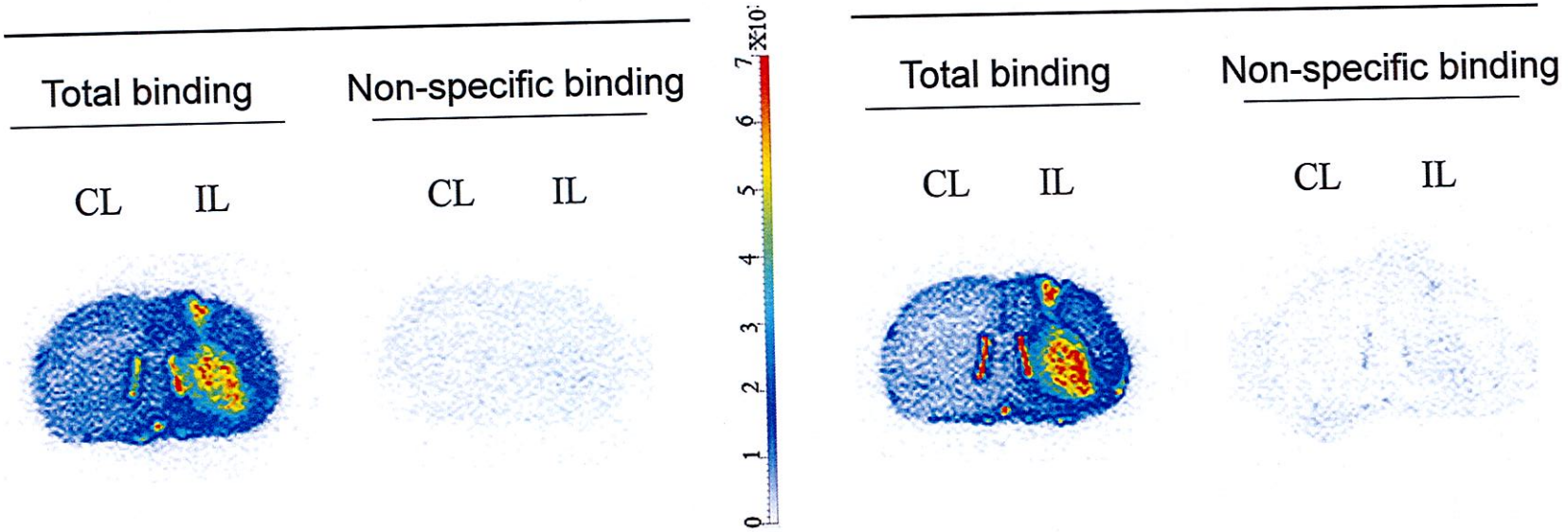
Total binding
Non-specific binding
CL
IL
CL
IL
x10
0
1
2
3
4
5
6
7
Total binding
Non-specific binding
CL
IL
CL
IL

B

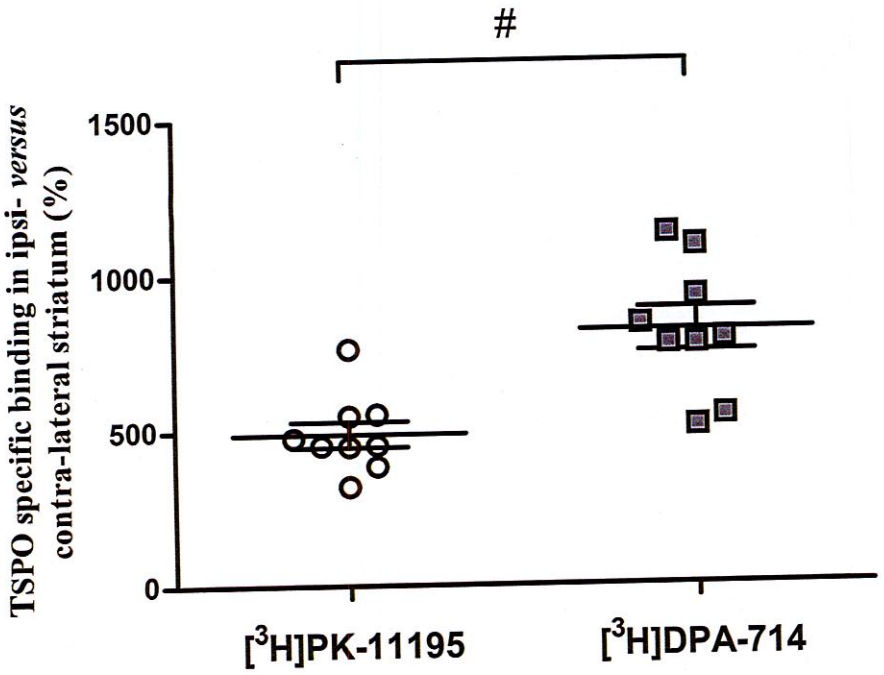
#
TSPO specific binding in ipsi- versus contra-lateral striatum (%)
1500
1000
500
0
[3H]PK-11195
[3H]DPA-714

C

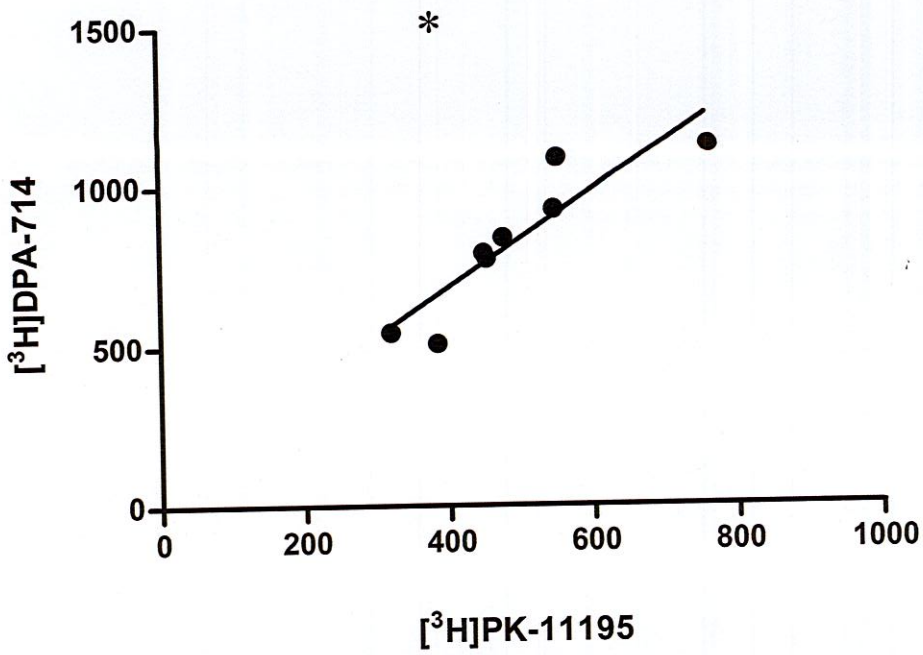
*
[3H]DPA-714
1500
1000
500
0
0
200
400
600
800
1000
[3H]PK-11195

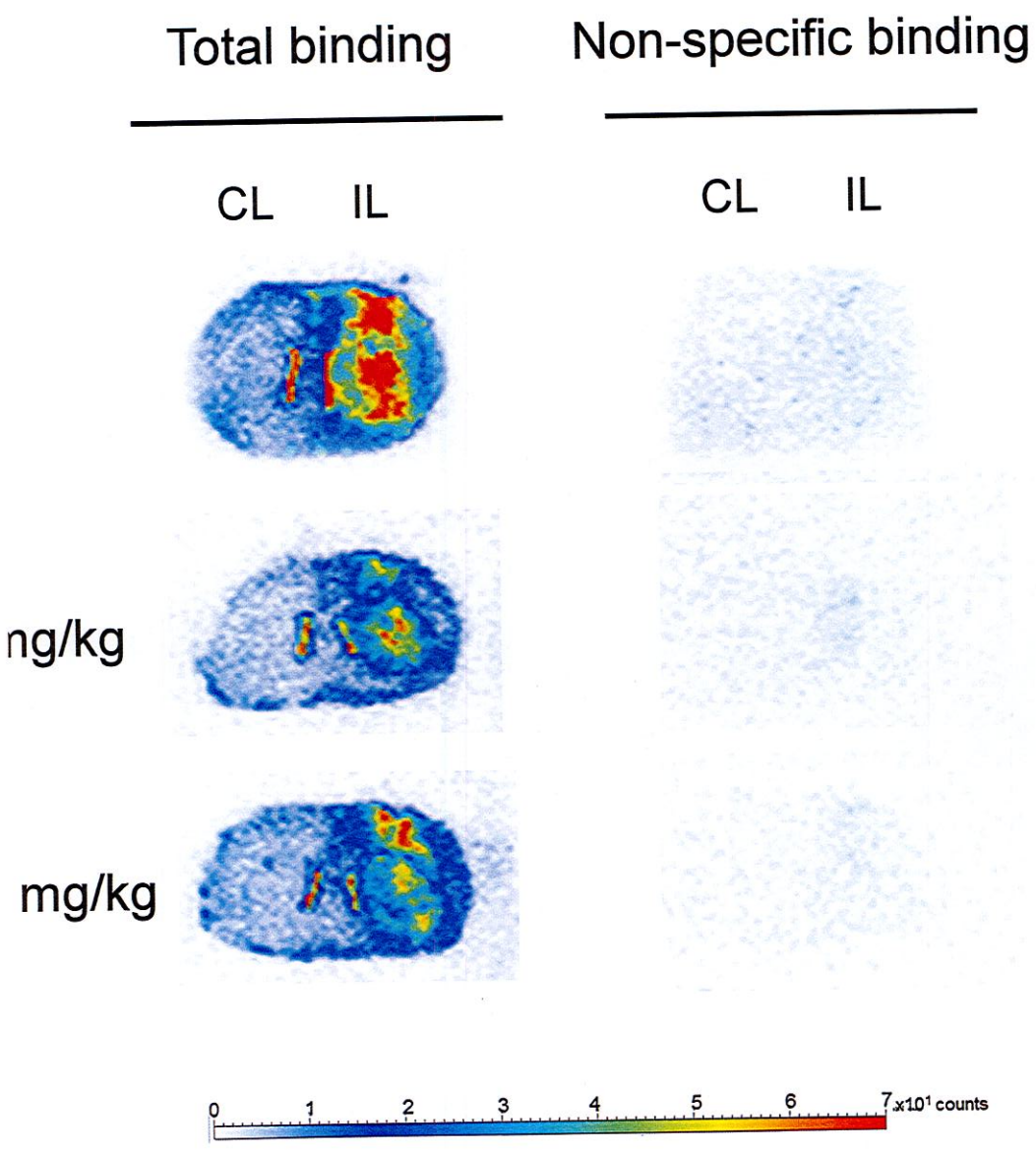
Total binding
Non-specific binding
CL
IL
CL
IL
ng/kg
mg/kg
0
1
2
3
4
5
6
7
x10¹ counts

B

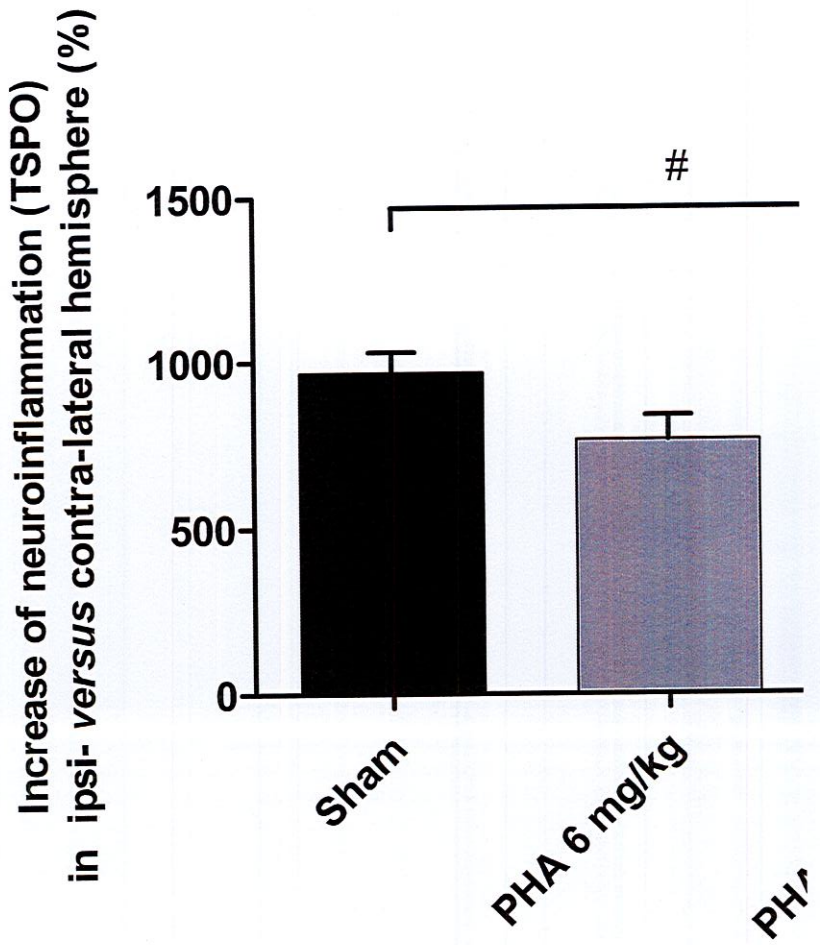
Increase of neuroinflammation (TSPO)
in ipsi- versus contra-lateral hemisphere (%)
#
1500
1000
500
0
Sham
PHA 6 mg/kg
PHA

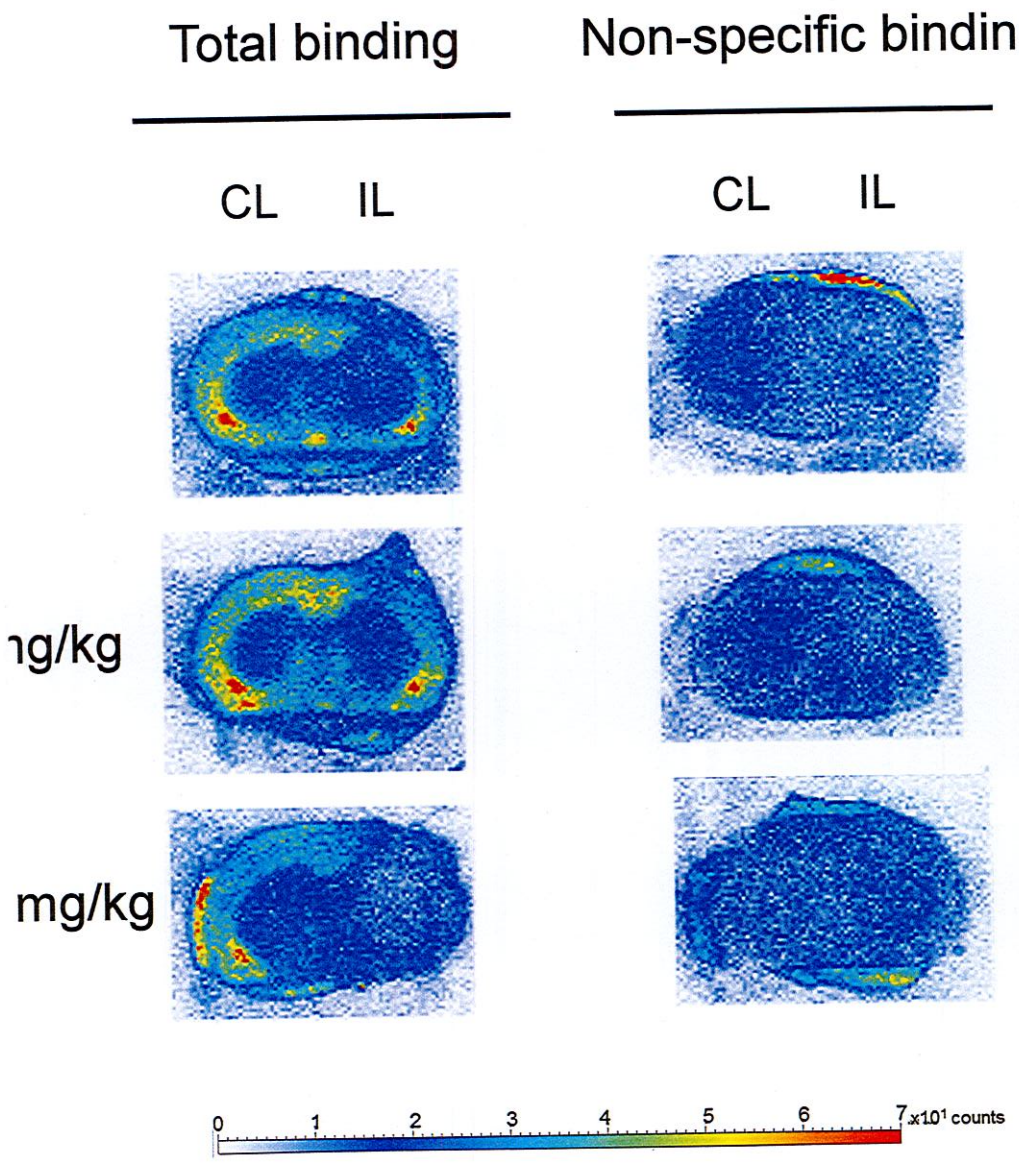
Total binding
Non-specific binding
CL
IL
CL
IL
ıg/kg
mg/kg
0
1
2
3
4
5
6
7
x10¹ counts

B

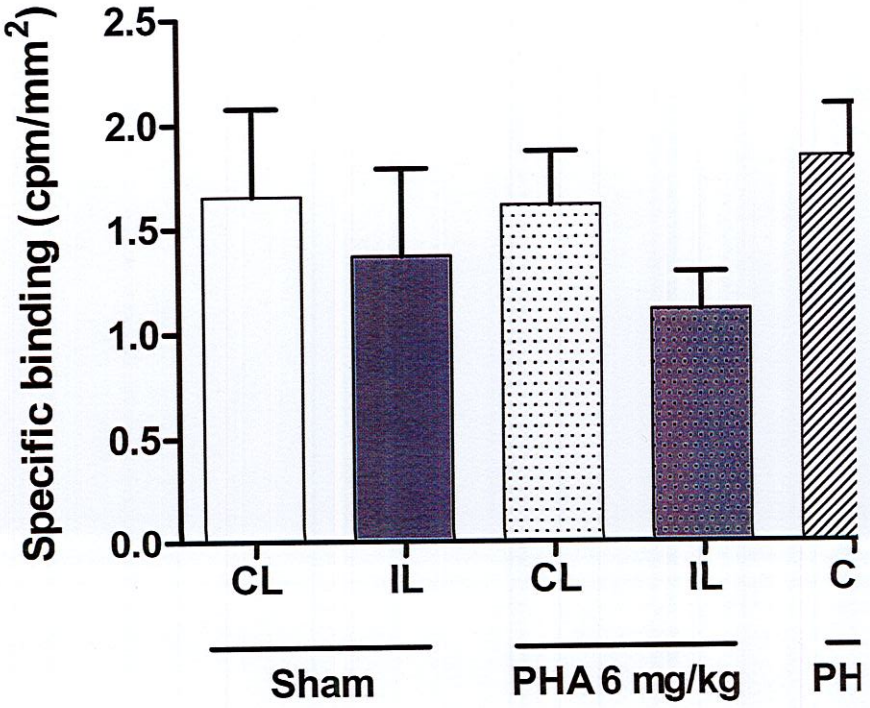
Specific binding (cpm/mm²)
2.5
2.0
1.5
1.0
0.5
0.0
CL
IL
CL
IL
C
Sham
PHA 6 mg/kg
PH

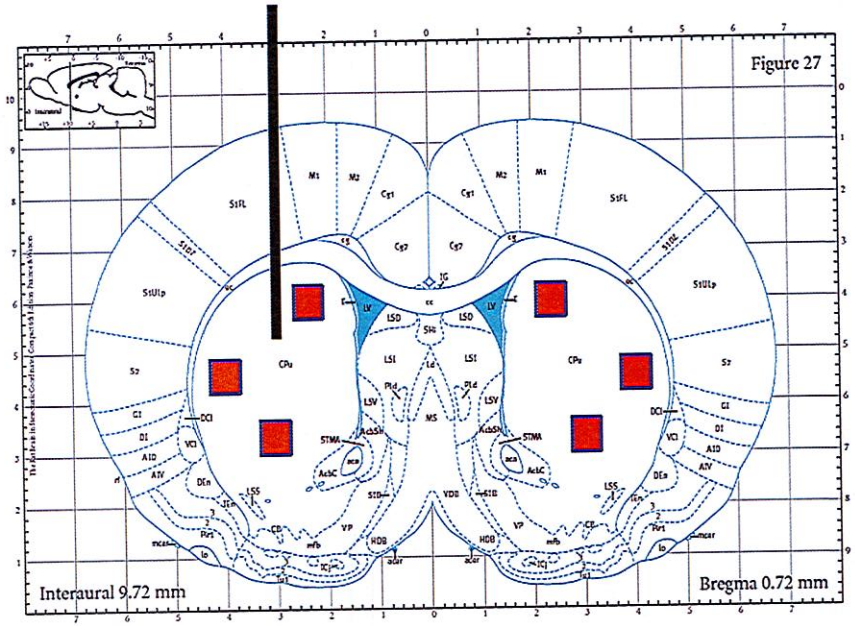
Figure 27
Interaural 9.72 mm
Bregma 0.72 mm

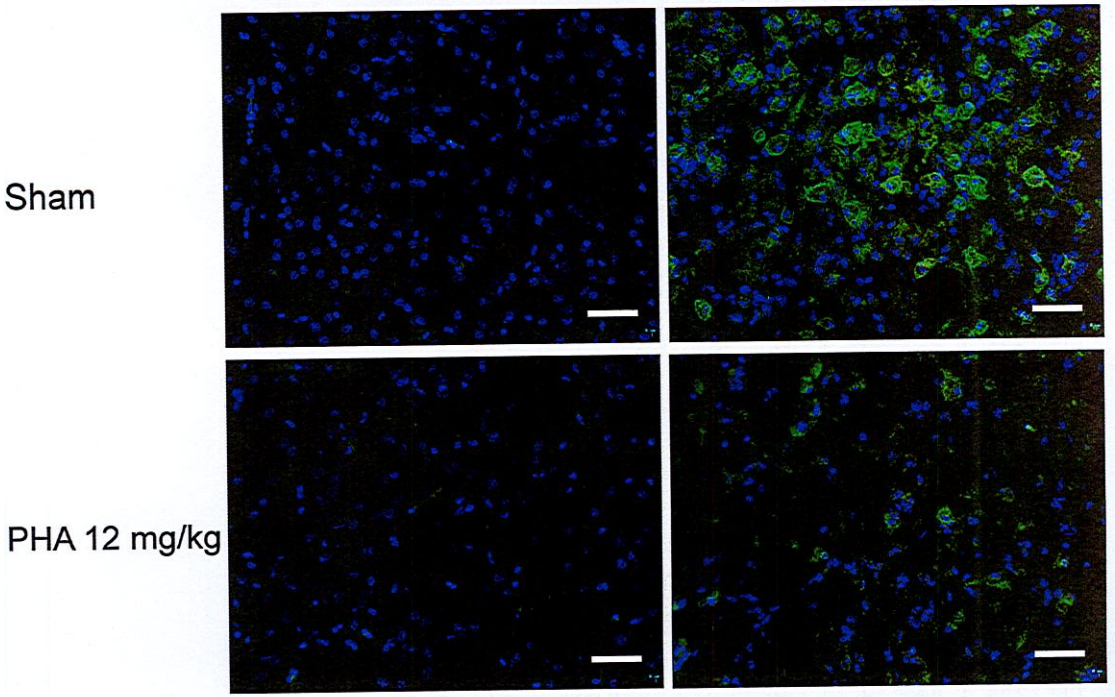
Sham
PHA 12 mg/kg

C

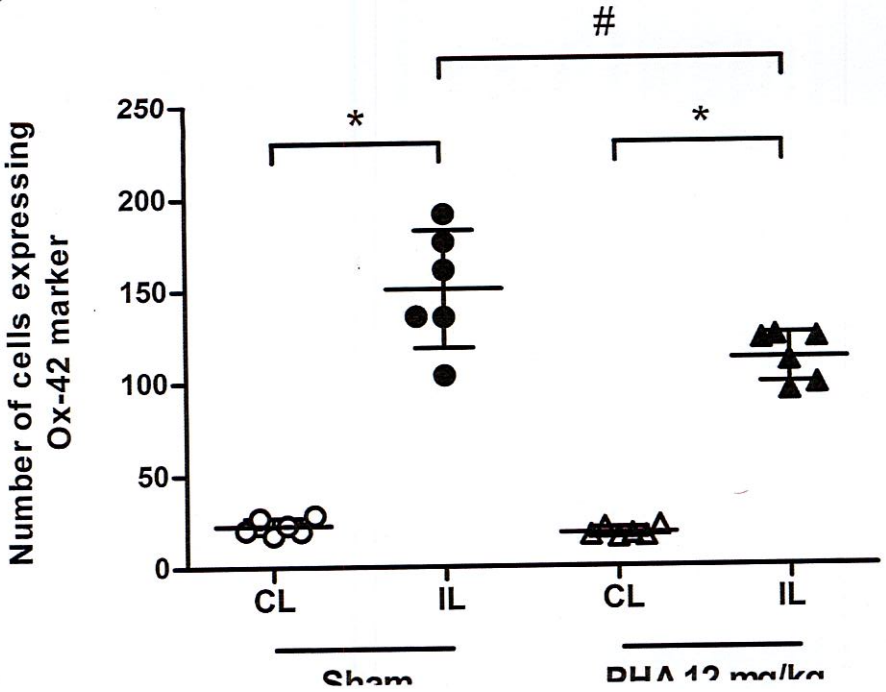
Number of cells expressing Ox-42 marker
250
200
150
100
50
0
*
*
#
CL
IL
CL
IL
Sham
PHA 12 mg/kg

D

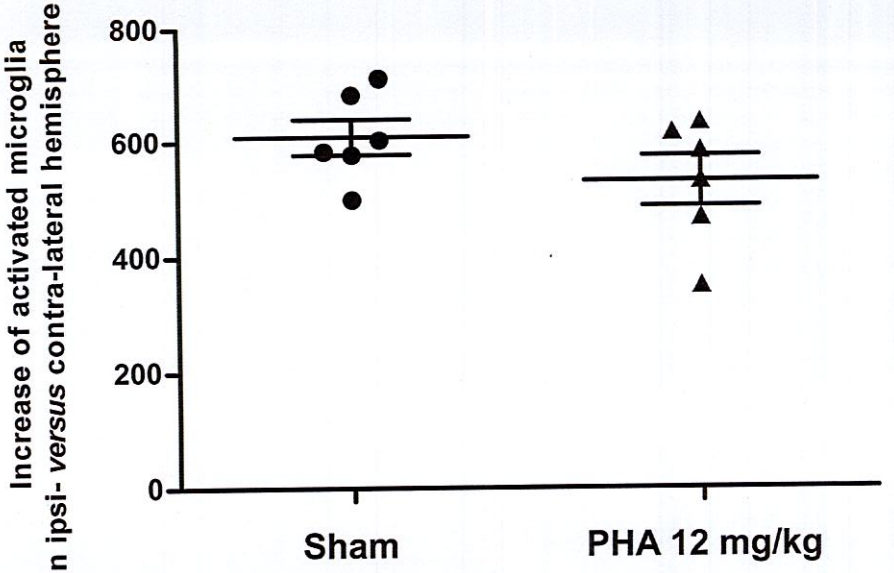
Increase of activated microglia in ipsi- versus contra-lateral hemisphere (%)
800
600
400
200
0
Sham
PHA 12 mg/kg

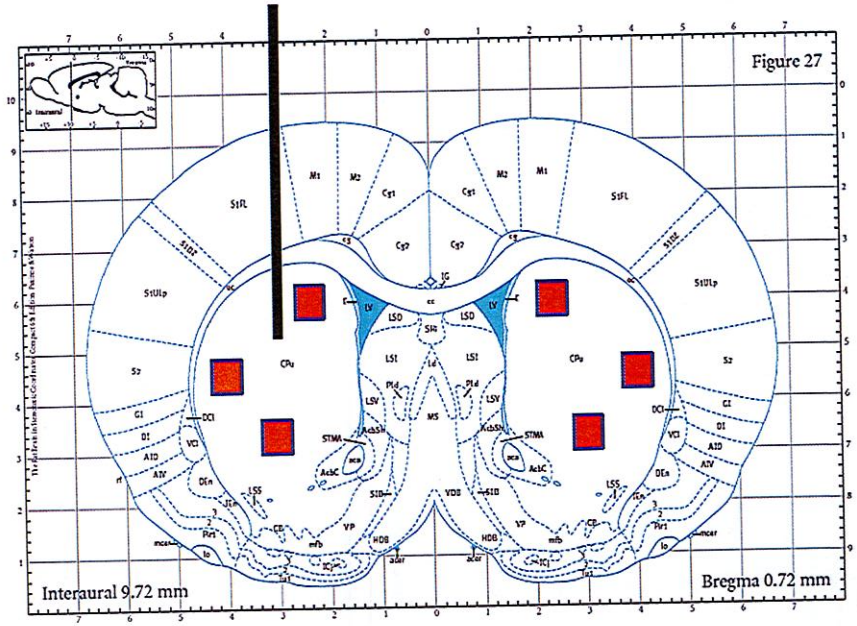
Figure 27
Interaural 9.72 mm
Bregma 0.72 mm

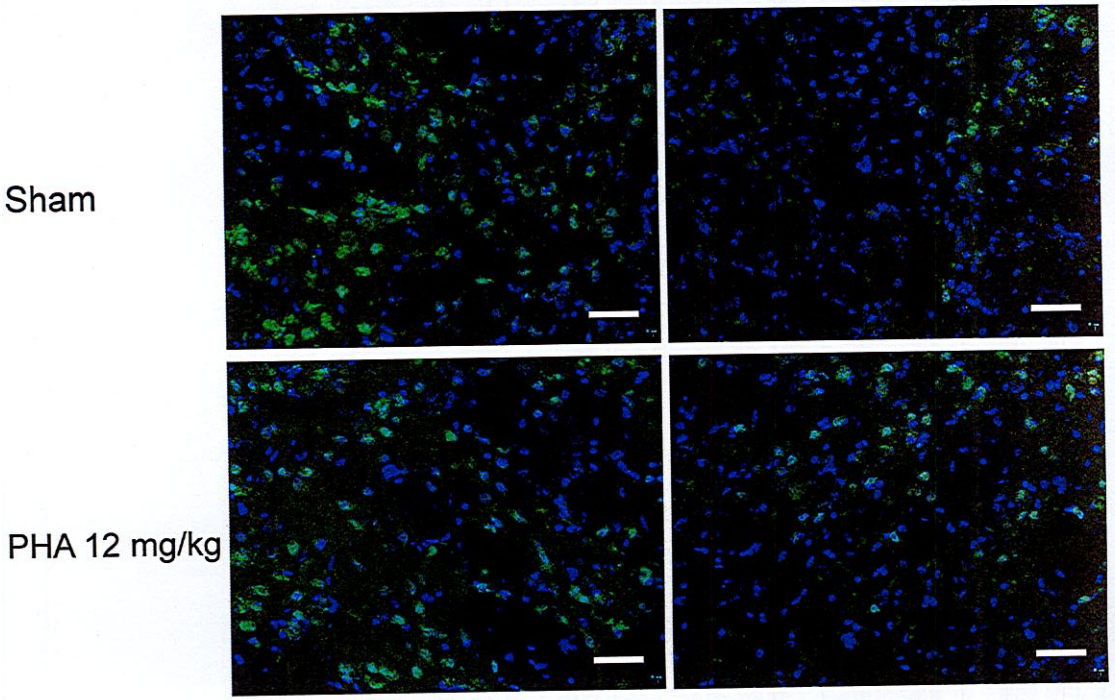
Sham
PHA 12 mg/kg

C

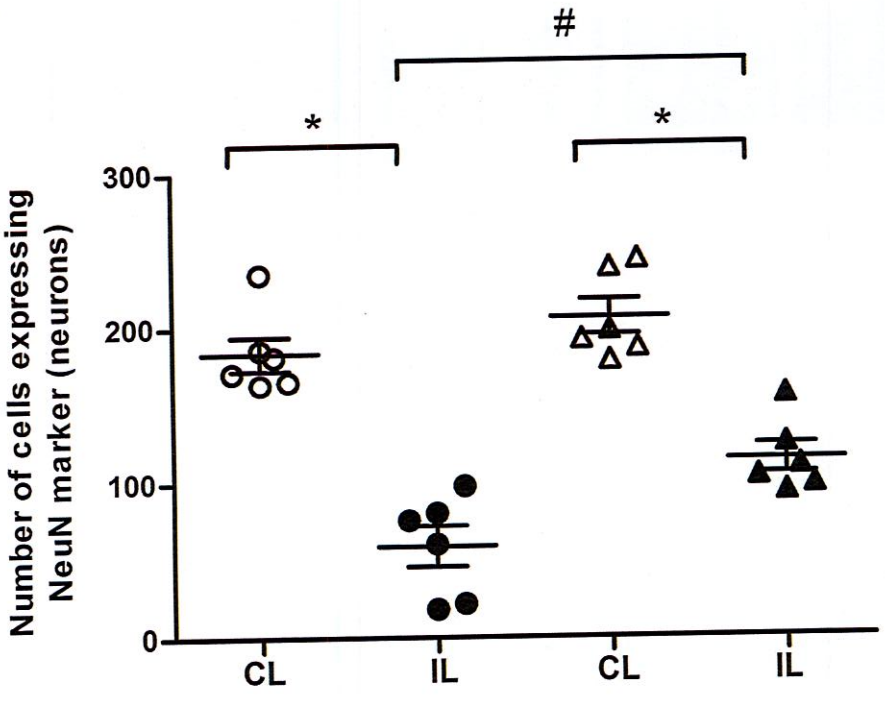
#
*
*
Number of cells expressing NeuN marker (neurons)
300
200
100
0
CL
IL
CL
IL

D

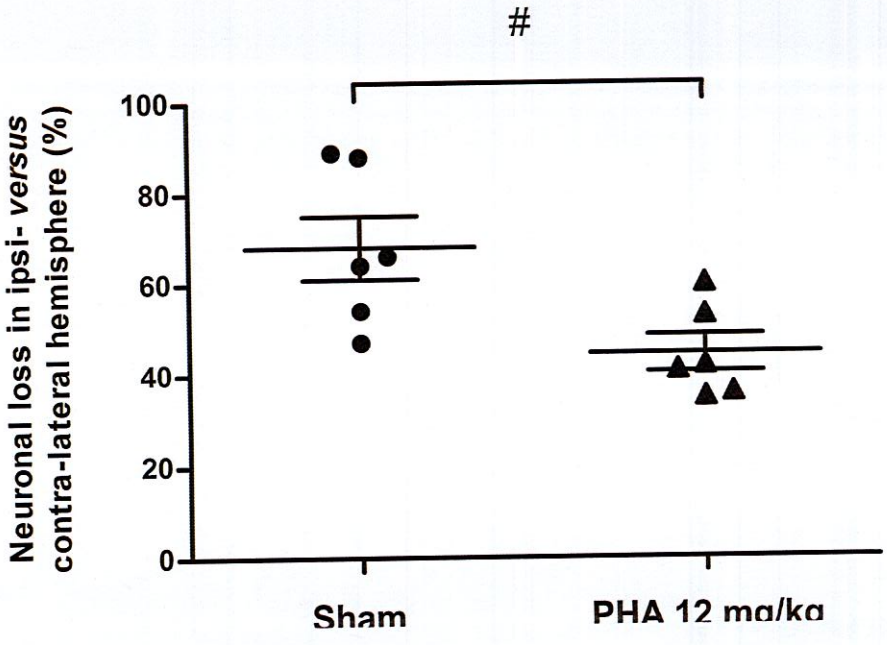
#
Neuronal loss in ipsi- versus contra-lateral hemisphere (%)
100
80
60
40
20
0
Sham
PHA 12 mg/kg